JPPIPA 10(12) (2024)

Jurnal Penelitian Pendidikan IPA

Journal of Research in Science Education

http://jppipa.unram.ac.id/index.php/jppipa/index

Application of Ground Penetrating Radar (GPR) Method for Evaluation of Sediment Structure in Paleotsunami Geopark Development Area, Aceh Besar, Indonesia

Salsa Nazia Putri[1], Nazli Ismail[*1,2,3], Muksin Umar[1,3]

[1] Master Program in Physics, Physics Departement, Universitas Syiah Kuala, Banda Aceh, Indonesia.
[2] Research Center Ethnosciences, Universitas Syiah Kuala, Banda Aceh, Indonesia.
[3] Tsunami and Disaster Mitigation Research Center, Universitas Syiah Kuala, Banda Aceh, Indonesia

Received: October 18, 2024
Revised: November 24, 2024
Accepted: December 26, 2024
Published: December 31, 2024

Corresponding Author:
Nazli Ismail
nazli.ismail@usk.ac.id

DOI: 10.29303/jppipa.v10i12.9464

Abstract: Ek Leuntie Cave is a karst cave in Meunasah Lhok, Lhoong District, Aceh Besar Regency. This cave is very rare. It has 12 tsunami layers dating back 7500 years. These layers need to be preserved as a paleotsunami geopark in Aceh. However, there are many challenges to developing public facilities in karst areas, such as sinkholes and landslides. Therefore, this study aims to investigate the potential hazards in the area by using the Ground Penetrating Radar (GPR) method at 700 MHz and 250 MHz frequencies. The GPR method is used because of its ability to image shallow subsurface structures with high resolution. The GPR method was used on 7 survey lines around Ek Leuntie Cave. The resulting radargrams are then processed using GPRPy software to clarify the reflection signal. GPR interpretation at 700 MHz and 250 MHz frequencies produces the same radargram at a very shallow depth, but the boundaries between layers are clearer at 700 MHz. Core data from multiple samples supports GPR interpretation. Based on the core data, the compact layer is located in the sandy soil layer, while the less compact layer is located in the old main road before the tsunami layer and in the bedrock. The less compact layer has potential hazards such as subsidence. The area is located in the west to south of the cave. Based on the GPR radargrams obtained, the investigation area is dominated by clay fill, sandy soil, clayey sand and bedrock. The results of the study are expected to be used as a reference for mitigation in the development of the Ek Leuntie Cave Geopark.

Keywords: Geopark; GPR; Karst; Paleotsunami; Sediment

Introduction

An earthquake in the Indian Ocean on 26 December 2004 triggered a massive tsunami that killed more than 165,000 people (BNPB, 2012). Aceh was the most severely affected area by the tsunami, making Aceh world-renowned. This natural disaster led the Aceh government, supported by several foreign countries, to build several tsunami-related sites, such as the Aceh Tsunami Museum and the "Aceh Thanks the World" Memorial Park. Curiosity about this tragedy fuelled the emergence of tsunami tourism (Nazaruddin & Sulaiman, 2013; Williamson, 2009). These sites are educational centers and symbolic reminders of the 2004 tsunami.

The form buildings and tsunami sites can also be natural areas such as parks. Geoparks are protected areas with distinctive geology where sustainable development is pursued, including tourism, conservation, education and research related to geology and other relevant sciences (Herrera-Franco et al., 2021). The geopark is developed through a bottom-up process, and the community must be a key stakeholder as this process requires a strong commitment to protect the geological heritage in the area (UNESCO, 2023). One of the historical geological sites that can be used as a

How to Cite:
Putri, S. N., Ismail, N., & Umar, M. (2024). Application of Ground Penetrating Radar (GPR) Method for Evaluation of Sediment Structure in Paleotsunami Geopark Development Area, Aceh Besar, Indonesia. *Jurnal Penelitian Pendidikan IPA*, *10*(12), 10627–10635. https://doi.org/10.29303/jppipa.v10i12.9464

geopark is Ek Leuntie Cave, Gampong Meunasah Lhok, Lhoong District, Aceh Besar Regency.

Twelve layers of ancient tsunami deposits were discovered by (Rubin et al., 2017) in Ek Leuntie Cave. The cave holds complete tsunami records, not only from the 2004 tsunami but also from tsunamis thousands of years ago. In addition, the site needs to be studied by future generations. Therefore, since 2019, Ek Leuntie Cave has been designated as a geopark site (Amri et al., 2022). By making Ek Leuntie Cave a conservation area, it is hoped that it can become a forum for scientific development and introduce Gampong Meunasah Lhok, Lhoong District, Aceh Besar Regency as a tourist area (Patria, 2019).

Gampong Meunasah Lhok, Lhoong District, Aceh Besar Regency, where Ek Leuntie Cave is located, has a distinctive geology in the form of karst areas (Bennett et al., 1981). Karst areas have many fractures in sedimentary rocks in limestone that compose karst areas, so they have large pores, high permeability, and high degrees of rock dissolution (Ford & Williams, 2007). These conditions cause problems in karst areas, such as slow soil formation speed, weak water storage capacity, and easy soil loss (Chen et al., 2022; Zhou et al., 2020). Therefore, it is necessary to protect the cave by detecting the subsurface karst conditions early and accurately. These conditions can play an important role in the environmental risk assessment of Ek Leuntie Cave.

One of the geophysical methods that can be used for karst areas is the Ground Penetrating Radar (GPR) method. GPR can adjust the antenna frequency according to the purpose of the survey used GPR with 200 MHz and 250 MHz center frequency antennas. With these frequencies, the results obtained are deep enough, up to 9 m, so that they can reach all parts of the limestone bedrock. The information is very valuable in the geotechnical field for building foundations in karst areas. For the higher frequency of 700 MHz, (Le & Nguyen, 2021) have already tested it but for underground pipeline purposes. The result is a high-resolution imaging of subsurface structures showing underground constructions with a depth of 0.5-0.75 m that can help maintain underground pipelines. From the various uses of frequency mentioned, it can be understood that frequency depends on the ultimate goal of the survey.

The GPR tool does not need to inject anything during data collection. The GPR tool only needs to be pushed, and data will be recorded from the rotating wheels so that this method does not damage the environment of the research area (Iftimie et al., 2021; Tešić et al., 2021). Therefore, the GPR method will be used in this study to look at the subsurface conditions of the karst area around Ek Leuntie Cave. In this study, the frequencies used are 250 MHz and 700 MHz. This is because, in addition to deeper layers, shallower layers are also important in supporting geopark development (Ambrosanio et al., 2019).

So far, studies inside Ek Leuntie Cave have been conducted and found ancient tsunami deposits in the cave, as many as 12 layers from 7400 years ago (Rubin et al., 2017). In addition to inside the cave, a review of the environment outside the cave has been conducted using the ERT method and the GPR method. Measurements with the Wenner-Schlumberger configuration ERT method were carried out by (Kurniawan, 2023) and (Khatimah et al., 2024). The results of the two researchers found that the foundation depth that could be recommended for geopark development was 4-8 m deep. Meanwhile, measurements with the GPR method by (Nanda et al., 2024) only used one trajectory oriented towards the cave and focused on studying subsurface structures. For the research results to identify potentially vulnerable areas, conducting GPR measurements with 7 trajectories scattered around the cave is necessary to identify karst features more accurately based on dielectric properties (Berezowski et al., 2021). It is expected that the GPR method can complement the results of the ERT method that was carried out. Therefore, subsurface information using the GPR method is needed for safety and comfort as a risk assessment in sustainable geopark management. This research aims to provide a more comprehensive understanding of the subsurface conditions around the cave so that it can support the planning of safe and sustainable infrastructure development in the geopark area. Effective risk mitigation efforts can be made by accurately identifying karst features, such as determining safe locations for constructing visitor facilities and evacuation routes.

Method

The data were collected in the coastal areas of Lhok Village, Lhoong, Aceh Besar Regency, Aceh. Data measurement was carried out on 7 lines. The purpose of measuring data in 7 lines is to cover all areas of the Geopark development, so 7 lines represent the area. A GPR instrument with an IDS Opera Duo series dual-frequency antenna (250 and 700 MHz) was used to conduct the survey.

Data Acquisition

During the data acquisition phase at the survey site, the tool is prepared in advance by connecting the laptop to the GPR via a USB cable to display the radargram along the survey track. Before running the GPR, the project name is determined to make it easier to sort the data. The antenna frequencies used in this study were 250 MHz and 700 MHz. The common offset

configuration was used. The GPR is driven by pushing only. When pushing the tool, it is ensured that the speed is constant to obtain accurate data. The GPR is pushed along 7 lines, as shown in Figure 1.

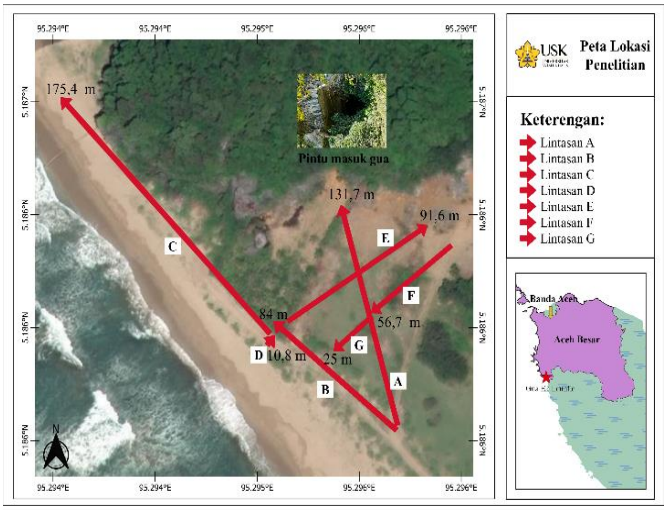

Figure 1. Measurement lines

Data Processing

Before the data can be processed, it undergoes a crucial step-conversion. A data converter is employed to transform the data into a format that can be read by the GPRPy data processing software. This step is essential as it sets the stage for the subsequent processing steps. The data obtained reveals that the number of samples/traces is 512, with a sampling time of 80 ns. From this, we can calculate that the sampling rate in the data is 6.4 GHz, indicating a high-quality radargram despite its shallow penetration depth.

The data processing stage consists of static correction, dewow, removal of mean trace, gain, velocity analysis depth conversion, and fk migration.

a. Static correction aims to restore the signal correctly at the first reflection event on the ground. This happens because there is a time lag before the signal hits the ground. With this correction, we can ensure that we record the exact time when the signal first bounced off the ground. This correction is very important to get a clear and accurate picture of the underground rock layers.
b. Dewow is a key step in the data processing stage that enhances the quality of the GPR data. Early DC and low-frequency signals often contaminate GPR data. These signals can arise due to various factors, such as the saturation of the measuring instrument when the first wave arrives or the influence of the cables used. The dewow process is designed to remove these unwanted signal components. Removing DC and low-frequency signals can improve the overall data quality and get a clearer picture of the subsurface structure.
c. Background removal is a data processing step that improves signal quality by removing unwanted background components. GPR data often has a persistent background signal, even when there is no reflected object. Various factors, such as interference from the surrounding environment or noise from the measuring instrument, can cause this background signal. The background removal process is specifically designed to remove these background signal components. By removing the background signal, we can improve the overall data quality and more easily identify the signal coming from the object we seek.
d. The deeper the signal penetration into the ground, the greater the attenuation. Various factors, such as soil conductivity, permittivity, and signal frequency, cause this. As a result, the amplitude of the reflected signal from a deep object will be weaker compared to an object close to the surface. To solve the signal attenuation problem, we need to increase the amplitude of the weak reflected signal. Gain is a signal amplifier, so the weak signal from depth can increase amplitude. Thus, we can detect objects that are buried deeper. The type of gain used in this research is time-power gain.
e. Velocity analysis is performed by fitting the hyperbola curve on the radargram to estimate the velocity value of the EM wave. A hyperbola velocity analysis is required to convert the cross-section to a depth scale. A hyperbola velocity analysis can be performed on any section containing diffraction or reflection hyperbola by matching the hyperbola function defined by velocity to the shape of the data.
f. Fk migration improves spatial resolution and correct subsurface reflector positions. This stage converts the data from the depth-distance domain to the frequency-wavenumber (fk) domain, applies migration correction and converts the data back to the spatial-time domain with a Fourier transform. Once the data is in the fk domain, migration correction is applied to correct for skewed or diffracted reflector positions in the data. Migration aims to focus the energy from the reflection to the correct location in the subsurface. Once the migration correction is applied, the data is converted back to the depth-distance domain using the inverse Fourier transform.

Result and Discussion

Track A is a track measured from south to northwest along 131.77m. In Figure 2, the top of the radargram still has a small air effect after static

correction. This is because there is no direct contact between the GPR and the ground surface, so a gap and air are still being recorded (Neal, 2004). The air effect in the radargram remains due to variations in ground level, so there is still some air even though it has been statically corrected.

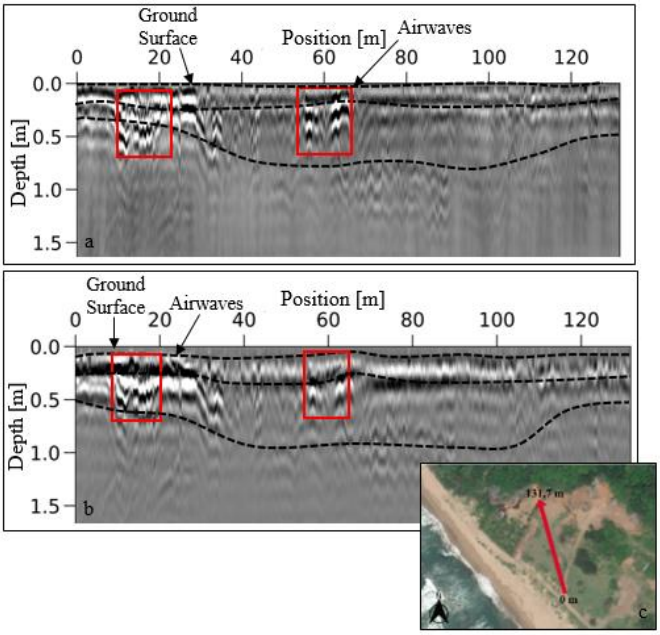

Figure 2. Radargram interpretation of a) 700 MHz frequency and b) 250 MHz frequency on line A. (c) measurement line A

In Figure 2, the radargram interpretation of line A shows three layers at a depth of 1.5m. Based on the drill data (Khatimah et al., 2024), the first layer in Figure 2 is interpreted as clay fill, the second layer as fine to coarse sand with variable water content and the third layer as limestone bedrock. There is a spike in the signal amplitude at approximately 10-30m and 55-65m in the red color box, resulting in a stronger signal than the others. The increase is thought to be due to a higher water content than the surrounding area or could be the roots of growing plants (Walia et al., 2021). This is supported by the field conditions during data collection. It can be seen that many thistle plants are growing thickly, so the tool has to be pulled from the front when pushing, and there are also puddles in several places.

Track B is a track measured from southeast to northwest over 84 m. As with the radargram on track A, there are still visible airwaves on the radargram on track B. In Figure 3, the interpretation of the radargram on track B shows three layers at a depth of 1.5m. Based on the drill data obtained by (Khatimah et al., 2024), the first layer at 0-0.3 m depth is interpreted as a clay fill. The second layer at a depth of 0.3-0.7 m is interpreted as wet sand, which is coarse-textured and contains gravel. The third layer, at a depth of 0.7-1.5m, is interpreted as a layer of limestone bedrock.

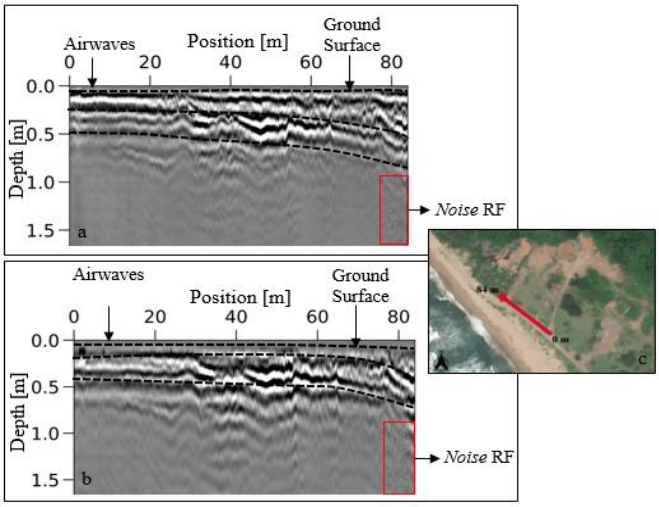

Figure 3. Radargram interpretation of a) 700 MHz frequency and b) 250 MHz frequency on line B. (c) measurement line B

Track C is a southeast-to-north-west track 175.44 m long. This track was taken along the coast close to the karst rocks that make up the cave wall. In Figure 4.11, the radargram interpretation of track C shows three layers of 1.5 m depth. In Figure 4, based on the drill data, the first layer is interpreted as beach sand from 0-38m and mountain rock rubble from 38-175.44m. The second layer is interpreted as a pre-2004 tsunami asphalt road layer with a mixture of sand and cave wall collapse. The third layer is interpreted as the hard rock that made up the old road.

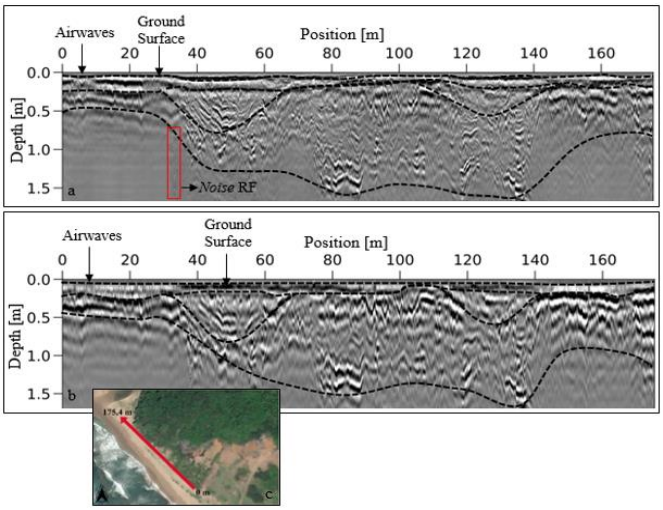

Figure 4. Radargram interpretation of a) 700 MHz frequency and b) 250 MHz frequency on line C. (c) measurement line C

Track D was measured from south-west to north-east for 10.85 m. Track D is the shortest track measured from the coast into the field. In Figure 5, the interpretation of the radargram on line D shows two layers at a depth of 0.4 m. The radargram obtained in Figure 5 shows that the signal pattern is similar to that

of track C. The first layer is beach sand, and the second layer is hard rock, which makes up the 2004 tsunami road, but not as much as in track D. The first layer is beach sand, and the second layer is hard rock, which makes up the 2004 tsunami road. Similar to the previous track, the 700 MHz frequency radargram in section a is sharper than the 250 MHz frequency radargram in section b (Salih & AL-hameedawi, 2017).

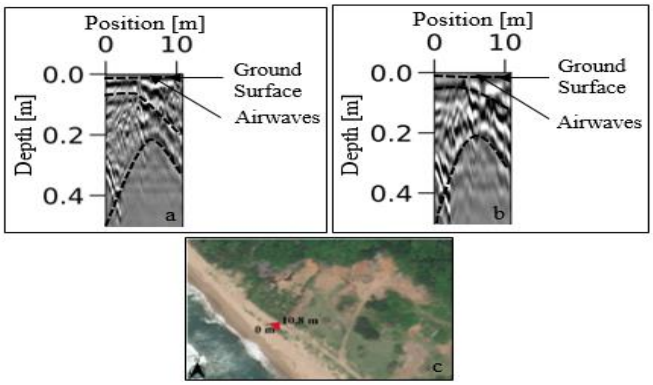

Figure 5. Radargram interpretation of a) 700 MHz frequency and b) 250 MHz frequency on line D. (c) measurement line D

Track E is a southwest-to-northeast track of 91.63m, in the same direction as track D. In Figure 4.13, the radargram interpretation of track E shows three 1.5m deep layers. In Figure 6, in sections a and b at 0-0.3 m, horizontal reflectors are visible on the surface. This is thought to be a water table. This is supported by the presence of a waterhole at a distance of 45-55 m, as indicated by the red box. However, the horizontal reflector in Figure 6, Part A, appears thicker than in Part B. In Figure 6, parts a and b, there is a red box showing the difference in signal amplitude before and after a distance of 45-55m. This is due to the presence of water puddles during measurements in the field, so the tool is lifted, and the signal looks like Figure 6.

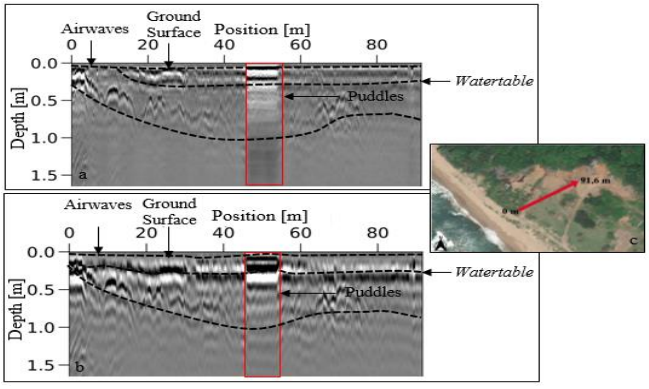

Figure 6. Radargram interpretation of a) 700 MHz frequency and b) 250 MHz frequency on line E. (c) measurement line E

Track F is measured from the northeast to the southwest along 56.76m. In Figure 7, the radargram interpretation on track F shows three layers of 1.5 m depth. Based on the drill data obtained by (Khatimah et al., 2024), the first layer from a depth of approximately 0-0.2 m is interpreted as fill, the second layer from a depth of 0.2-0.6 m is interpreted as fine to coarse clay sand with variable water content, and the third layer is interpreted as limestone bedrock. Between the first and second layers is thought to be the water table. This was also encountered in the previous cross-section E.

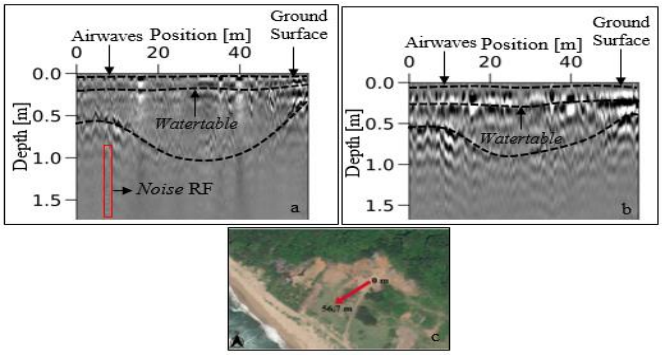

Figure 7. Radargram interpretation of a) 700 MHz frequency and b) 250 MHz frequency on line F. (c) measurement line F

Track G is a 25 m long track from north-east to south-west. In Figure 4.15, the radargram interpretation on track G shows three layers of 1.5 m depth. Based on auger data, the first layer from a depth of about 0-0.2 m is interpreted as filled soil, the second layer from a depth of 0.2-0.4 m is interpreted as fine to coarse sand with varying water content, and the third layer is interpreted as limestone bedrock. In Figure 8, the 700 MHz frequency radargrams have clearer interlayer boundaries than the 250 MHz frequency radargrams. The echo effect is most evident in the 250 MHz frequency radargram. From the interpretation results obtained on traces A, E, F and G, it can be concluded that the field in front of the cave has been filled in the upper part.

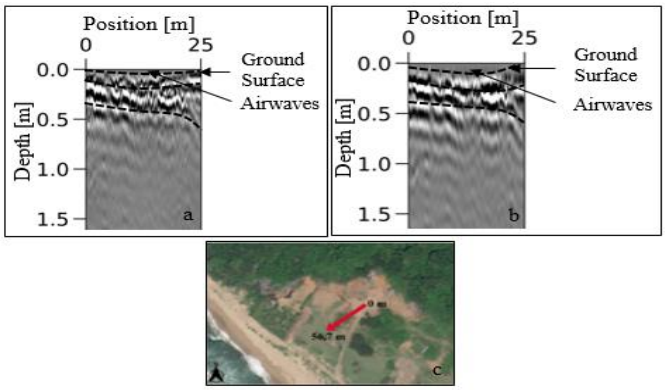

Figure 8. Radargram interpretation of a) 700 MHz frequency and b) 250 MHz frequency on line G. (c) measurement line G

GPR measurements, a key tool in our understanding of the subsurface, were carried out to

determine the dielectric constant of the layer based on the velocity of electromagnetic waves. The measurement uses 7 tracks, as shown in Figure 3.1. The measurement position on track A aims to determine the distribution or continuity of Ek Leuntie Cave. Measurements on track B aim to determine the structure in the out-of-field area of the cave. Measurements on track C aim to determine the structure near the cave wall. Measurements on tracks D and E aim to determine the structure in the cave field intersecting track A so that the meeting point between tracks A and E can be a validation between tracks. Measurements on tracks F and G aim to determine the structure in the cave field.

The black and white pattern in a GPR radargram represents the amplitude of the strength of the radar wave reflections from different layers and objects below the ground. High amplitudes (strong black or white colors on the radargram) indicate strong reflections. This is due to significant dielectric contrast, which increases the amplitude of the reflection (Maas & Schmalzl, 2013).

The condition of track A on the surface at 0-27 m distance is a sandy area, and at 27-131 m distance is a landfill. On the radargram of track A, there are strong reflections and high amplitudes at a distance of 0-28 m and 58-62 m. It is suspected that there is more water content at these positions, which is supported by the condition of track A on the surface. It is suspected that there is more water content at these positions, which is supported by the condition of track A on the surface. High humidity areas have a higher dielectric constant and can be identified by the strong reflection amplitude on the radargram (Van Dam, 2014).

Track B shows a clear contrast between the upper and lower layers. Based on the drill data, the upper layer is sandy soil, and the lower layer is bedrock. The sandy soil layer has a high amplitude reflection, which is considered susceptible to seawater intrusion. Track B was measured close to the coastline, making seawater intrusion possible.

The first section of Track C on the surface is sandy soil from 0-35 m, mountain rock rubble from 35-140 m and a mixture of sandy soil and mountain rock rubble. Based on the boring data, the layer below track C is the layer that made up the asphalt road before the 2004 tsunami, and the third layer is the hard rock that made up the road. Judging from the measurement location of trace C, this trace shows the continuation of trace B, although it was not measured continuously due to the presence of vegetation. The strongest amplitude reflection is in the area of the sandy soil. On the other hand, the high amplitude reflection on the former tarmac road before the tsunami is thought to come from the voids of the former asphalt road before the tsunami.

Track D, the shortest track, continues track E. Judging from the amplitude reflection pattern, the subsurface structure is the same as track C, but the dominant layer is the pre-2004 tsunami asphalt roadbed.

Track E intersects Track A at points 45 and 90 meters apart. At the intersection of tracks E and A, the layers are the same, namely clay fill. However, there is a depression at the bottom of layer E, which is thought to be the water table layer. The increase in amplitude on the radargram clearly shows the water table layer.

Like track E, track F also has a water surface layer in its subsurface. However, at the top of the radargram of track F, the irregular increase in amplitude is thought to be due to the presence of voids in the layer. The amplitude increase is more significant at a distance of more than 40 m, suggesting a higher water content in this area compared to other areas in track F.

Finally, track G, still continuous with track F, has a clear layer of increased amplitude due to the dielectric constant contrast. This area is thought to be susceptible to seawater intrusion. However, it could also be rainwater trapped in the clay layer of the fill.

Sandy soils have larger particles than clay soils. This causes water to flow more quickly in sandy soils, preventing water from pooling on the surface. In contrast, the clay infill's particle size is smaller, so the water remains on the surface. Puddles at several points in the field during data collection support this. The radargram records this difference in moisture variation as a dielectric constant contrast (Van Dam, 2014).

The presence of a high dielectric contrast indicates that the area is vulnerable. Low-density materials, such as sandy soils, are less able to support large surface structures or infrastructure than denser clays (Saarenketo, 2006). Therefore, building on sandy soils is not recommended for future Geopark development. If you want to build on the area, you will need to fill it with clay to make it stronger to support infrastructure, and you will also need to do further research.

As the study site is close to the sea, the high dielectric contrast is thought to be due to seawater intrusion. Seawater has a much higher dielectric constant than freshwater or dry soil, so a high amplitude reflection is recorded on the radargram, indicating the boundary between freshwater and saltwater. Areas prone to seawater intrusion are located on tracks A, B, and C at the beginning and end of the track, as well as G. On track G, it could be due to rainwater; this is supported by the seasonal conditions at the time of data acquisition, which is the rainy season.

Interpreting the 700 MHz and 250 MHz GPR on all tracks produced the same radargram at shallow depths, but the boundaries between layers were clearer at 700 MHz. Figures 9 and 10 show the merging of all tracks, both at 700 MHz and 250 MHz frequencies.

Figure 11 shows the planned design of the future geopark development. Supporting facilities will be built

around the cave, including the main entrance, car park, miniature cave, toilet, museum building, garden, cave access door, pond and evacuation route. The location of the GPR acquisition conducted in this study coincides with the geopark development area, so the study results can be used as a consideration for an early warning system against geological disaster threats in the area to be developed. According to Indonesian Government Regulation No. 26/2008, karst ecosystems are recognized as geologically protected areas in landscapes and essential ecosystems requiring special attention.

The results of this study on the effectiveness of geopark development can be interpreted in different ways. Areas with wet sand are not recommended for development, as low-density sand layers can increase disaster vulnerability. In addition, sites with voids are not recommended.

Unsafe locations and not recommended for development based on the BPBA design are in Zones C, E, F and G, where there are areas of dry to wet sand at the surface to a depth of more than 1 meter, but deeper areas of hollow rock containing water-infiltrated sand or holding groundwater. This area is generally found in the zone above the bedrock, where this layer has a high dielectric constant contrast.

The safest area for constructing support facilities is around the cave entrance and the cave. This site is located in the northern part, in zone N (cave entrance) and zone O (pond), extending from the west to zone K in the east. It is a dense zone with a relatively hard rock composition. It is more stable and less prone to ground movement or structural collapse.

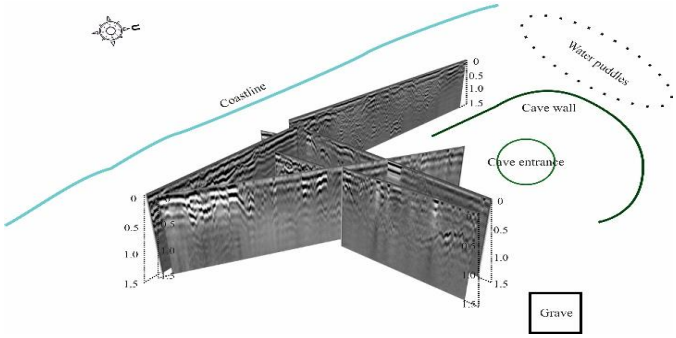

Figure 9. Combination of all 700 MHz radargrams

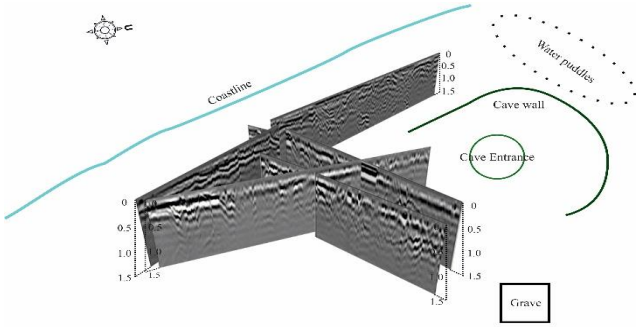

Figure 10. Combination of all 250 MHz radargrams

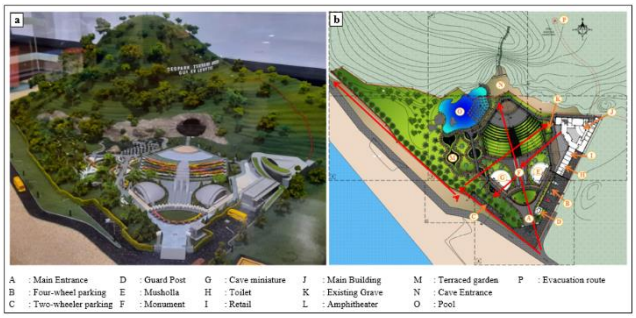

Figure 11. Development planning design of the Ek Leuntie Cave Paleotsunami Geopark a) Mock-up of the Ek Leuntie Cave Paleotsunami Geopark b) Design view with measurement track (BPBA, 2019)

Conclusion

A clay fill layer, a sandy soil layer, a clayey sand layer and a limestone bedrock layer dominate the subsurface structure in the study area. These layers are found in tracks A, B, E, F and G, while the asphalt road layer dominates tracks C and D. The characteristics of the soil layers in the Ek Leuntie Cave karst area, based on reflections in the GPR radargram, show differences in density between the soil layers. Based on the drill data, the low-density layer is in the sandy soil layer, and the high-density layer is in the asphalt road layer and limestone bedrock. Based on the characteristics of the soil layer, several areas have been identified that could cause potential hazards if development plans are implemented. The potential hazard that could be caused is subsidence under heavy loads. Potentially hazardous areas based on the BPBA design are to the west to the south of the cave.

Acknowledgments

The authors would like to thank LPPM USK for funding this research through the Student Thesis Research grant and the Tsunami and Disaster Mitigation Research Centre (TDMRC) for facilitating the use of GPR equipment during data measurement.

Funding

This research was funded by Penelitian Tesis mahasiswa (PTM), grant number 389/UN11.2.1/PG.01.03/SPK/PTNBH/2024 and "The PTM was funded by LPPM USK".

Conflicts of Interest

The authors declare no conflict of interest.

References

Ambrosanio, M., Bevacqua, M. T., Isernia, T., & Pascazio, V. (2019). The Tomographic Approach to Ground-Penetrating Radar for Underground Exploration

and Monitoring: A more user-friendly and unconventional method for subsurface investigation. *IEEE Signal Processing Magazine*, *36*(4), 62–73.

Amri, W., Ismail, N., & Dewi, C. (2022). Pembuatan dan Penggunaan Replika Sedimen Tsunami Purba untuk Media Pembelajaran Tsunami. *Jurnal IPA & Pembelajaran IPA*, *6*(4), 393–408. https://doi.org/10.24815/jipi.v6i4.27274

Bennett, J. D., McC Bridge, D., Cameron, N. R., Djunuddin, A., Ghazali, S. A., Jeffrey, D. H., Kartawa, W., Keats, W., Rock, N. . M. S., Thomson, S. J., & Whandoyo, R. (1981). *Geologic map of the Banda Aceh Qudrangel, Sumatra*.

Berezowski, V., Mallett, X., Ellis, J., & Moffat, I. (2021). Using ground penetrating radar and resistivity methods to locate unmarked graves: A review. *Remote Sensing*, *13*(15), 1–22. https://doi.org/10.3390/rs13152880

BNPB. (2012). *Masterplan Pengurangan Risiko Bencana Tsunami*.

Chen, F., Bai, X., Liu, F., Luo, G., Tian, Y., Qin, L., Li, Y., Xu, Y., Wang, J., Wu, L., Li, C., Zhang, S., & Ran, C. (2022). Analysis Long-Term and Spatial Changes of Forest Cover in Typical Karst Areas of China. *Land*, *11*(8), 1–20. https://doi.org/10.3390/land11081349

Ford, D., & Williams, P. (2007). Karst Hydrogeology and Geomorphology. In *Karst Hydrogeology and Geomorphology*. John Wiley & Sons. https://doi.org/10.1002/9781118684986

Herrera-Franco, G., Montalván-Burbano, N., Carrión-Mero, P., Jaya-Montalvo, M., & Gurumendi-Noriega, M. (2021). Worldwide research on geoparks through bibliometric analysis. *Sustainability (Switzerland)*, *13*(3), 1–32. https://doi.org/10.3390/su13031175

Iftimie, N., Savin, A., Steigmann, R., & Dobrescu, G. (2021). Underground pipeline identification into a non-destructive case study based on ground-penetrating radar imaging. *Remote Sensing*, *13*(17). https://doi.org/10.3390/rs13173494

Khatimah, H., Kurniawan, F., Ismail, N., Umar, M., Munir, B., Asyqari, A., Pramana, A. H., & Afrizal, T. (2024). *Electrical Resistivity Tomography (ERT) untuk menginvestigasi struktur bawah permukaan kawasan karst di area Gua Ek Leuntie , Provinsi Aceh Electrical Resistivity Tomography (ERT) for investigating subsurface structures in the karst area of the Ek Leu*. *12*(4), 6–12. https://doi.org/10.24815/jacps.v12i4.35860

Kurniawan, F. (2023). *Identifikasi Struktur Bawah Permukaan Menggunakan Metode Electrical Resistivity Tomography (ERT) di Sekitar Gua Ek Leuntie Kecamatan Lhoong Kabupaten Aceh Besar*. Universitas Syiah Kuala.

Le, C. V. A., & Nguyen, T. V. (2021). *Ground penetrating radar attributes analysis for detecting underground artificial structures in urban areas , Vietnam*. *22*(2), 249–257.

Maas, C., & Schmalzl, J. (2013). Using pattern recognition to automatically localize reflection hyperbolas in data from ground penetrating radar. *Computers and Geosciences*, *58*(February), 116–125. https://doi.org/10.1016/j.cageo.2013.04.012

Nanda, M., Ismail, N., Mahlia, M., Amril, F., Munir, B., Asyqari, A., Khatimah, H., & Haditiar, Y. (2024). Application of ground-penetrating radar for shallow subsurface investigation at the coastal area of lhok village, lhoong, aceh besar regency, aceh. *BIO Web of Conferences*, *87*. https://doi.org/10.1051/bioconf/20248702015

Nazaruddin, D. A., & Sulaiman, R. (2013). Introduction to "TSUNAMI TOURISM": Notes from Aceh, Indonesia. *International Journal of Sciences*, *2*(03), 71–81. https://www.ijsciences.com/pub/article/160%0Ahttps://doi.org/%0Ahttps://www.ijsciences.com/pub/pdf/V2-201303-16.pdf

Neal, A. (2004). Ground-penetrating radar and its use in sedimentology: Principles, problems and progress. *Earth-Science Reviews*, *66*(3–4), 261–330. https://doi.org/10.1016/j.earscirev.2004.01.004

Patria, H. T. (2019). *Puncak Peringatan 15 Tahun Tsunami Aceh di Pidie: Melawan Lupa, Membangun Siaga*. Serambinews. https://aceh.tribunnews.com/2019/12/26/puncak-peringatan-15-tahun-tsunami-aceh-melawan-lupa-membangun-siaga

Rubin, C. M., Horton, B. P., Sieh, K., Pilarczyk, J. E., Daly, P., Ismail, N., & Parnell, A. C. (2017). Highly variable recurrence of tsunamis in the 7,400 years before the 2004 Indian Ocean tsunami. *Nature Communications*, *8*(1), 1–12. https://doi.org/10.1038/ncomms16019

Saarenketo, T. (2006). *Electrical properties of road materials and subgrade soils and the use of Ground Penetrating Radar in traffic infrastructure surveys*.

Salih, M. M., & AL-hameedawi, A. N. M. (2017). The Effect of the Different Frequency on Skin Depth of GPR Detection. *Journal of Babylon University/Engineering Sciences*, *25*(2), 2017.

Tešić, K., Baričević, A., & Serdar, M. (2021). Non-destructive corrosion inspection of reinforced concrete using ground-penetrating radar: A review. *Materials*, *14*(4), 1–20. https://doi.org/10.3390/ma14040975

UNESCO. (2023). *UNESCO Global Geoparks*. https://www.unesco.org/en/iggp/geoparks/about

Van Dam, R. L. (2014). Calibration Functions for

Estimating Soil Moisture from GPR Dielectric Constant Measurements. *Communications in Soil Science and Plant Analysis*, *45*(3), 392–413. https://doi.org/10.1080/00103624.2013.854805

Walia, A., Rastogi, R., Kumar, P., & Jain, S. S. (2021). Reviewing methods for determination of Dielectric Constant required to Calibrate GPR Study for Asphalt Layers. *IOP Conference Series: Materials Science and Engineering*, *1075*(1), 012026. https://doi.org/10.1088/1757-899x/1075/1/012026

Williamson, L. (2009). *Tsunami museum opens in Indonesia*. BBC News. http://news.bbc.co.uk/2/hi/7905770.stm

Zhou, L., Wang, X., Wang, Z., Zhang, X., Chen, C., & Liu, H. (2020). The challenge of soil loss control and vegetation restoration in the karst area of southwestern China. *International Soil and Water Conservation Research*, *8*(1), 26–34. https://doi.org/10.1016/j.iswcr.2019.12.001